Optical tweezers toolbox: better, faster, cheaper; choose all three

Alexander B. Stilgoe[a], Michael J. Mallon[b], Yongyin Cao[c], Timo A. Nieminen[a] and Halina Rubinsztein-Dunlop[a]

[a]School of Mathematics and Physics, The University of Queensland, Brisbane, Australia;
[b]Research Computing Center, The University of Queensland, Brisbane, Australia;
[c]Harbin Institute of Technology, Harbin, China

ABSTRACT

Numerical computation of optical tweezers is one path to understanding the subtleties of their underlying mechanism—electromagnetic scattering. Electromagnetic scattering models of optical trapping can be used to find the properties of the optical forces and torques acting on trapped particles. These kinds of calculations can assist in predicting the outcomes of particular trapping configurations. Experimentally, looking at the parameter space is time consuming and in most cases unfruitful. Theoretically, the same limitations exist but are easier to troubleshoot and manage. Towards this end a new more usable optical tweezers toolbox has been written. Understanding of the underlying theory has been improved, as well as the regimes of applicability of the methods available to the toolbox. Here we discus the physical principles and carry out numerical comparisons of performance of the old toolbox with the new one and the reduced (but portable) code.

1. INTRODUCTION

Traditionally, optical tweezers are though of as a single beam which produces optical gradient force trap when interacted with a spherical particle.[1] However, in recent times, single beam optical traps no longer typify the cutting edge of wet or soft condensed matter micro-scale research. Instead, multiple beam systems such as counter-propagating,[2,3] or multiple-beam systems are used.[4,5] These kinds of systems can provide enhanced detection[6] and control multiple traps, including their polarization[7] over micro-systems. However, even in the case of a simple double trap system, the motion of particles acting in an optical force field under thermal fluctuations are non-trivial, displaying many features inaccessible to single beam optical traps.[8] A result of the emergent properties of the system is that the precise behavior of even a simplistic multiple beam system cannot be completely reasoned without first making an observation of the effect. Computational methods provide a convenient alternative to performing optical tweezers experiments to discover these properties.[8–10] For continuous wave monochromatic radiation impinging on a dielectric sphere the macroscopic, time-harmonic Maxwell equations adequately capture the optical physics present on a microscopic, but not a nanoscopic, scale. The first publicly available tool set available for computation of trapping of symmetric microscopic particles was the optical tweezers toolbox[11] (available at http://www.physics.uq.edu.au/omg/Links.html). The toolbox originally ran on MATLAB (TM—The MathWorks, Inc.), but had neither speed optimization nor sufficient demonstration of capabilities to be considered for use in a number of optical tweezers problems. Its purpose was primarily to calculate the forces and torques on a single trapped particles with certain degrees of symmetry. It gives excellent quantitative agreement for optically trapped spheres[12] and for some non-spherical objects. Here we improve the optical tweezers toolbox from the ground up, from the basic theory, to how this theory abstracts to various observable phenomena in experiments. Part of this demonstration will involve comparisons between the newest version of the toolbox, the *free-er* portable version and the previous version (which was virtually unchanged from that used to produce results in Nieminen et al., 2007).

Further author information: (Send correspondence to T. A. Nieminen)
T. A. Nieminen: E-mail: timo@physics.uq.edu.au, Telephone: +617 3365 2422

Optical Trapping and Optical Micromanipulation IX, edited by Kishan Dholakia, Gabriel C. Spalding, Proc. of SPIE Vol. 8458, 84582E · © 2012 SPIE · CCC code: 0277-786/12/$18 · doi: 10.1117/12.929365

Downloaded From: http://proceedings.spiedigitallibrary.org/ on 12/09/2015 Terms of Use: http://spiedigitallibrary.org/ss/TermsOfUse.aspx

2. THEORY

The optical tweezers trapping problem, at its core, is one of electromagnetic scattering. As a result, all the methodologies used to solve scattering problems can also be applied to solve the trapping problem. In the case of spheres the scattering solution for monochromatic light is found by Lorenz–Mie theory.[13,14] Lorenz–Mie theory is a specific case of a set of theories called the Generalized Lorenz–Mie theories.[15] These theories can be used to calculate the effective scattering from any shape subject to the following condition: That there is only one point of intersection between a chosen point within the object and that objects' surface. These models can be adapted to polychromatic and pulsed light sources, but the optical tweezers toolbox assumes that the trapping radiation is monochromatic.

If we assume monochromatic radiation, the Maxwell equations reduce to the following expression:

$$\nabla \times \mathbf{A} + k^2 \mathbf{A} = 0 \tag{1}$$

where $\mathbf{A}$ can be either the magnetic or electric field. However, the general solutions (in the various coordinate systems) for this problem are infinite series solutions of trigonometric polynomial functions. In the spherical coordinate system, the two necessary solutions are labeled $\mathbf{M}$ and $\mathbf{N}$ and can be constructed out of the following special functions:

$$\psi\left(r,\theta,\phi\right) = j_n\left(r\right) L_n^m\left(\sin\theta\right) \exp\left(im\phi\right), \tag{2}$$

$$\mathbf{M}_{nm} = \hat{\mathbf{r}} \times \nabla\psi, \tag{3}$$

$$\mathbf{N}_{nm} = \frac{1}{k} \nabla \times \mathbf{M}_{nm}, \tag{4}$$

where j_n is a Bessel, Neumann or Hankel function, L_n^m the associated Legendre polynomial, $\mathbf{M}$ is the linearly independent solution for transverse electric (TE) modes and $\mathbf{N}$ is the linearly independent solution for transverse magnetic (TM) modes. As monochromatic radiation is made out of a superposition of transverse electromagnetic modes we can express an arbitrary electric field:

$$\mathbf{E} = \sum_{n=1}^{\infty} \sum_{m=-n}^{n} a_{nm}\mathbf{M}_{nm} + b_{nm}\mathbf{N}_{nm} \tag{5}$$

where a_{nm} and b_{nm} are complex weights for a particular mode. Most of the information about the field at the origin is in the low order modes ($n \to 1$), therefore one can truncate the expansion at a reasonable point and still be confident of good convergence within a finite region of space. Now that the basic foundation of the model has been discussed we now need to introduce the scatterers so that we can start investigating how optical tweezers trap particles. The scattering problem here is a boundary value problem of the macroscopic Maxwell equations. In general, we want to solve the following problem:

$$\hat{\mathbf{n}} \times \left(\sum_{n,m} a_{nm}\mathbf{M}_{nm}^{(3)} + b_{nm}\mathbf{N}_{nm}^{(3)} + p_{nm}\mathbf{M}_{nm}^{(1)} + q_{nm}\mathbf{N}_{nm}^{(1)} \right) = \hat{\mathbf{n}} \times \left(\sum_{n',m'} c_{n'm'}\mathbf{M}_{n'm'}^{\prime(3)} + d_{n'm'}\mathbf{N}_{n'm'}^{\prime(3)} \right), \tag{6}$$

$$\hat{\mathbf{n}} \times \left(\sum_{n,m} a_{nm}\mathbf{N}_{nm}^{(3)} + b_{nm}\mathbf{M}_{nm}^{(3)} + p_{nm}\mathbf{N}_{nm}^{(1)} + q_{nm}\mathbf{M}_{nm}^{(1)} \right) = \hat{\mathbf{n}} \times \left(\sum_{n',m'} m_c c_{n'm'}\mathbf{N}_{n'm'}^{\prime(3)} + m_c d_{n'm'}\mathbf{M}_{n'm'}^{\prime(3)} \right), \tag{7}$$

where a_{nm}, c_{nm}, and p_{nm} are the complex amplitudes of the incident, internal, and scattered TE fields, respectively. Likewise: b_{nm}, d_{nm}, and q_{nm} are the complex amplitudes of the incident, internal, and scattered

Downloaded From: http://proceedings.spiedigitallibrary.org/ on 12/09/2015 Terms of Use: http://spiedigitallibrary.org/ss/TermsOfUse.aspx

TM fields, respectively. **M** and **N** are the wavefunctions expressed in equations (3) and (4) on the surface of the object. The superscripts '(1)' and '(3)' denote whether the wavefunction uses Hankel (of the first kind) or Bessel functions. The dashes in expressions (6) and (7) distinguish between the use of distance parameters, $k'r$ and kr, for the particle and suspending medium, respectively. Clearly, this is a large linear system, but is fairly numerically stable for a large enough choice of surface points. The weights a_{nm} and b_{nm} are put into a matrix once found. This resulting transfer matrix[16] (or T-matrix) is a kind of scattering matrix used commonly in atmospheric science. The power of a T-matrix is that it can contain information necessary for repeated calculations. In the case of a sphere, a T-matrix representation is unnecessary as it will be a diagonal matrix of repeated elements due to its high degree of symmetry. As we know the same series expansion holds good for simple dielectrics. We no longer have to keep track of fields to know what the forces are. There are well defined relationships for the momentum of spherical waves.[17,18] From these relationships we can apply Newton's second law of motion to our scattering problem and therefore calculate optical forces acting upon the scatterer.

In addition to calculating the force at the origin one will also wish to find forces at other locations. For spherical waves there are analytical solutions for both translations and rotations. The rotation matrix produced by the toolbox does so by using a defined relation between the angular trigonometric functions which make up the wavefunctions.[19] Rotations are completely reversible using this method. Translations of the wavefunctions in the toolbox are done so using matrices generated from the recursions found in Videen.[20] Both the translation and rotation matrix formulations are technical and advanced in scope and provide little extra insight past the description made in this paragraph.

Given the tools listed above we can generate the forces and torques acting upon trapped dielectric particles at any point in space. The optical tweezers toolbox[11] has all of these required functions.

3. ROTATING AND TRANSLATING BEAMS

An observation was made during testing the old version of the optical tweezers toolbox. For highly focused beams, the translation of the beam in any direction had no negative impact on the local properties of the field at the origin. An example of this is shown in figure 1.

Figure 1(c) demonstrates an interesting property of translated beams: Provided that one can initially describe the entire beam and contain the particle in the truncation limit of basis functions, any translation from the origin will be valid for the beam–particle system. As a result, it is no slower to translate to distant points in space than local ones and get convergence in the truncation region. In the original toolbox this was not assumed and so the limiting factor in calculations was how far the beam needed to be translated from the origin. A rotation–translation combination using this method must always start from the origin because translations (but not rotations) are irreversible. The transformation to move the beam to a particular point in space is as follows in our formalism:

$$\mathbf{a}' = \mathbf{W}^{\dagger}(\theta,\phi)\left[\mathbf{A}(r)\,\mathbf{W}(\theta,\phi)\,\mathbf{a} + \mathbf{B}(r)\,\mathbf{W}(\theta,\phi)\,\mathbf{b}\right], \tag{8}$$

$$\mathbf{b}' = \mathbf{W}^{\dagger}(\theta,\phi)\left[\mathbf{A}(r)\,\mathbf{W}(\theta,\phi)\,\mathbf{b} + \mathbf{B}(r)\,\mathbf{W}(\theta,\phi)\,\mathbf{a}\right], \tag{9}$$

where $\mathbf{W}(\theta,\phi)$ is the Wigner D-matrix for vector spherical harmonics,[19] $\mathbf{A}(r)$ and $\mathbf{B}(\mathbf{r})$ are the vector translations of the wavefunctions,[20] $\mathbf{a}$ and $\mathbf{b}$ are respectively the TE and TM mode weights for the beam. The translated beam weights: $\mathbf{a}'$ and $\mathbf{b}'$ give the correct beam shape at the new location, subject to the choice of truncation. This truncation we parameterize with the number of radial basis functions, $N_{\max}$. To move to any point in space many recalculations of translation and rotation matrices must be made. A comparison of the time taken for the old and new methods along with their deviation is shown in figure 2. The grid for each calculation in figure 2 was 20^3 points the extent of each dimension being $[-(2r+0.7\lambda_{\text{med}}), 2r+0.7\lambda_{\text{med}}]$. The choice of the range was such that most of the trapping behavior of the particle was contained in the region. The choice of the number of radial basis functions (n) is shown on the figure as either a number below or above a data point. A minimum of $N_{\max} = 10$ was chosen, as this number of radial functions was required to describe the beam. Otherwise, the choice of $N_{\max}$ was determined from the particle size and translation distance (using the old method) and just

Downloaded From: http://proceedings.spiedigitallibrary.org/ on 12/09/2015 Terms of Use: http://spiedigitallibrary.org/ss/TermsOfUse.aspx

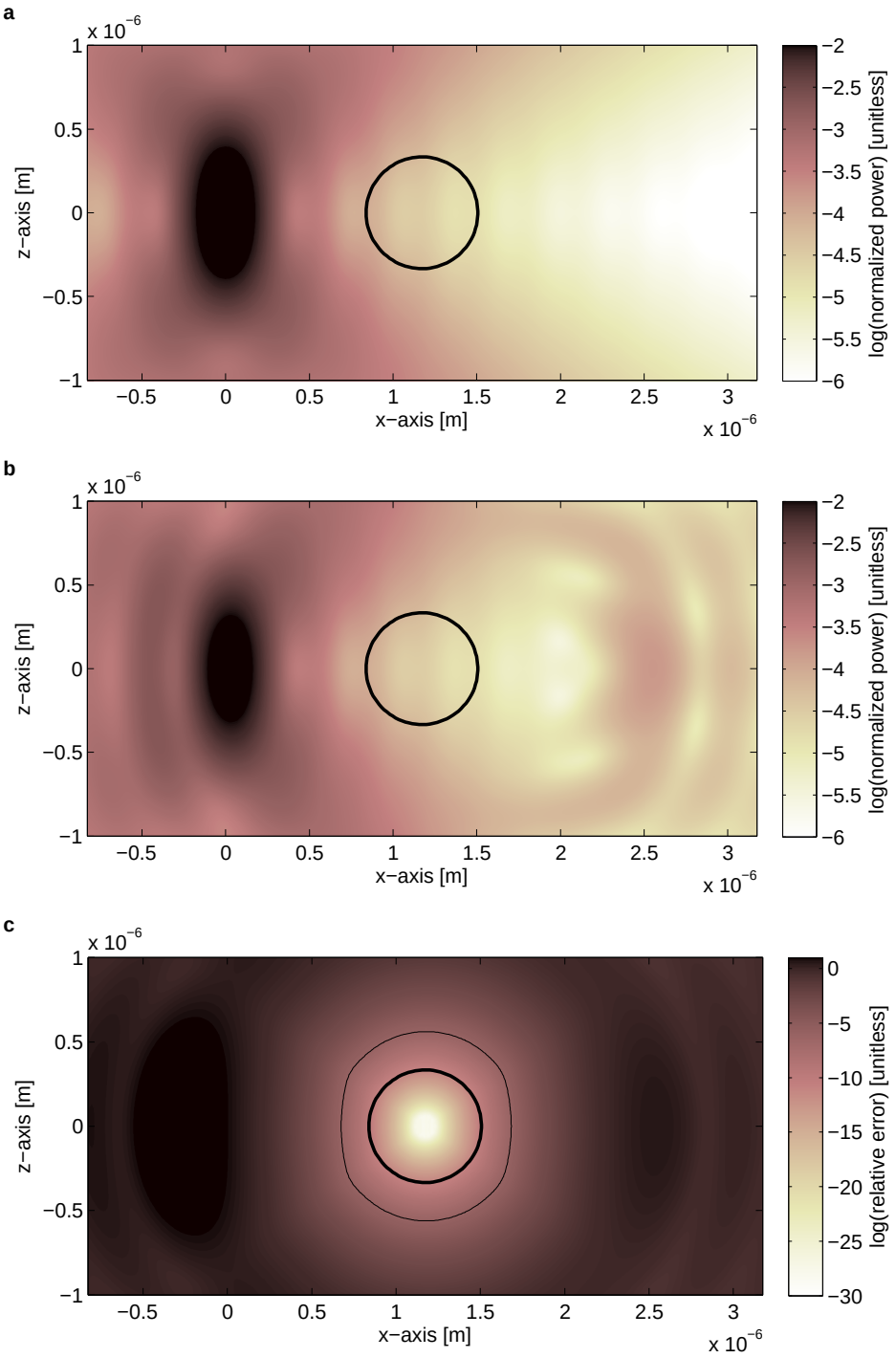

Figure 1. The intensity of an offset, moved and difference of a highly focused TEM_{00} mode at a wavelength of 790nm in air. The thick line in the three plots is the location for which our truncation converges. (a) The intensity of a TEM_{00} mode as calculated at the center of the coordinate system and offset on a grid to a location $2\lambda_{\mathrm{med}}$ from the origin. (b) The intensity of the same original beam calculated at the origin but then translated using the consequences of the vector translation theorem. (c) The difference in the offset and moved fields plotted as the relative error of an intensity normalized at the offset position. The error remains many orders of magnitude smaller than the intensity around this point. The thin line gives the contour with relative error of 10^{-6}.

Downloaded From: http://proceedings.spiedigitallibrary.org/ on 12/09/2015 Terms of Use: http://spiedigitallibrary.org/ss/TermsOfUse.aspx

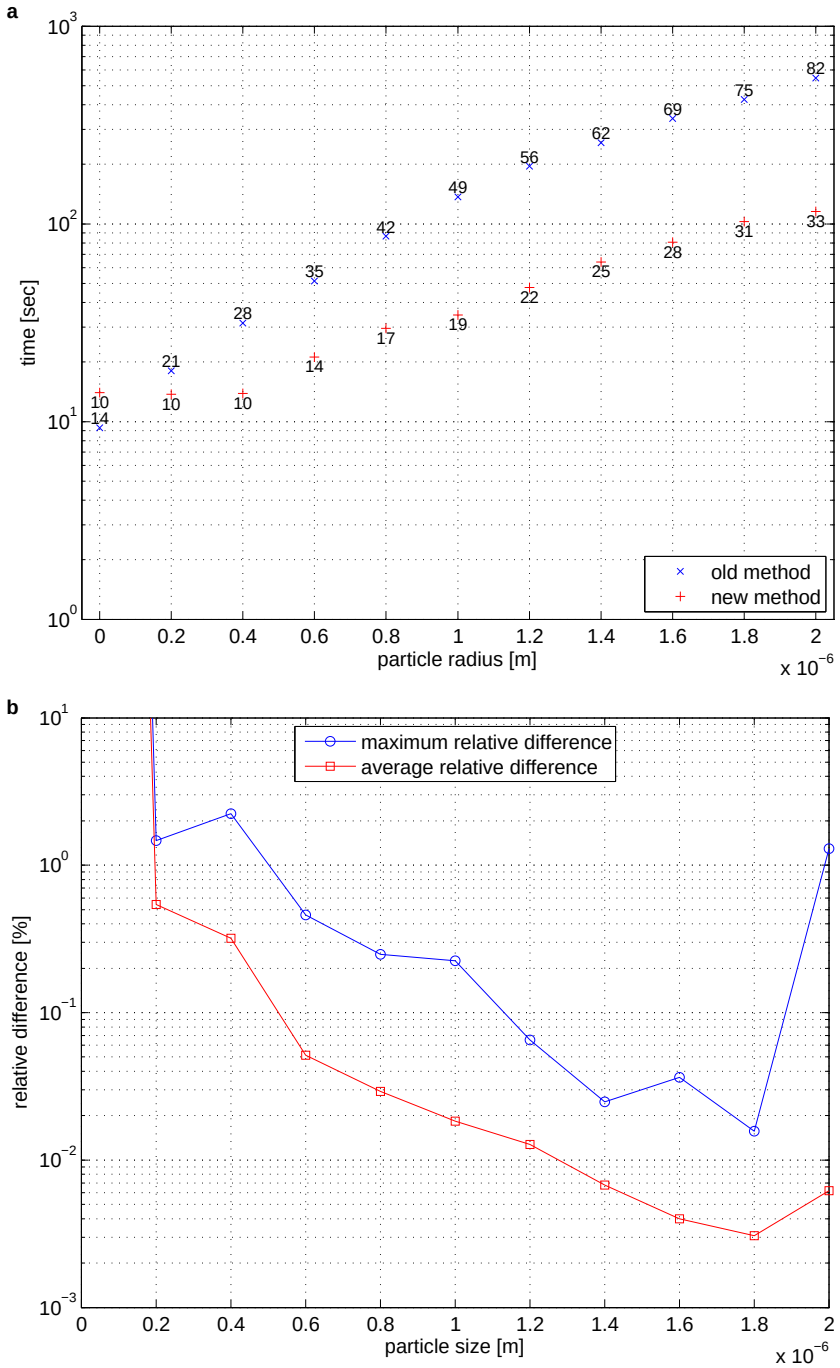

Figure 2. Comparison and analysis of the differences between the new and old methods of calculating force field grids for particles in the radius range of 10^{-12}m to 2×10^{-6}m. (a) The time taken to calculate a 20^3 grid over the bounds $[-(2r + 0.7\lambda_{\text{med}}), 2r + 0.7\lambda_{\text{med}}]$ in the x-, y- and z-axes for the old method ('$\times$') and the new method ('+'), the $N_{\max}$ for the functions are displayed above and below the relevant coordinates. (b) The maximum and average percentage difference normalized to the maximum value of force calculated on the grid using the new method. When the particle radius is 10^{-12}m, both methods are numerically unstable and produce wildly varying values at each grid point. All these differences are small compared to typical measurement errors.

Downloaded From: http://proceedings.spiedigitallibrary.org/ on 12/09/2015 Terms of Use: http://spiedigitallibrary.org/ss/TermsOfUse.aspx

particle size (using the new method). A regular grid in the principal directions is employed in both examples in figure 2(a). Both methods employ optimizations. As the calculation of translation matrices is the slowest part of the calculation for spheres, the regular grid was a great boon for performance in calculations at a large number of grid points. The beam would be offset in z by one of the pre-calculated translation matrices, rotated and translated separately in the x- and y- direction in succession yielding the appropriate beam translation. By being pre-calculated both the rotation and translation matrices greatly increased the speed of calculation. As a result, the calculation of scattering was simply a matter of repeated matrix multiplication followed by some arithmetic to find the force. The small number of basis functions using the new method in the toolbox means that a succession of pre-calculated matrices is no longer possible. However, as the calculation here is made on a regular grid it is possible to group together (up to dozens of) translation matrices so that for these particular distances from the origin the matrices don't have to be re-calculated. The rotation matrices must be calculated for each grid point because the sorting by translation length will change the ordering of the rotation matrices on a regular grid. This does not impact performance significantly because MATLAB can efficiently calculate rotation, but not the translation, matrices. Based on the data displayed in figure 2(a) the new method appears to be more speed optimized due to the reduced number of basis functions despite the increase in the number of calculations of translations and rotations. One can see the difference in efficiency due to the increased number of translations and rotations by comparing the time taken for the small particle calculations. We will find later that using the new method for multiple beams enhances the calculation, both in terms of the speed and potentially the accuracy at large particle sizes.

4. MULTIPLE BEAM OPTICAL TWEEZERS AND THE EFFECT OF BEAM COHERENCE

Multiple beam optical tweezers (the most common being dual beam) are now commonly used in investigations of microscopic systems. Multiple scattering from nearby particles and influences from nearby beams should be characterized to account for observations of trapping and hence measurement behavior. We will restrict ourselves to single particles localized in an environment of multiple beams. A detailed discussion of multiple scattering and its effects using the toolbox can be found in these proceedings. When one considers dual beam optical tweezers and asks the question: how many traps are formed by two beams? The intuitive answer is two. However, this is not always the case. Ignoring coherence, it is possible to create more than two traps with two beams.[8] The presence of these traps cannot be predicted with either the Rayleigh or dipole scattering theories. It is possible to predict with geometrical optics (ray tracing) models, but the model gets the details wrong. The reason that multiple traps can occur is due to the effect of the edge of a particle leaving the beam. Trapping forces for dipole scatterers decreases as the intensity gradient decreases. However, for particles larger than the beam waist a significant proportion of the particle still contains the beam even though the intensity gradient at the center of the particle begins to decrease. The particle therefore can still convert a large proportion of the beam momentum. As a consequence, particles near this location display physics not present in the dipole and Rayleigh models. Additionally, the geometrical optics models get the physics of this region wrong as it neglects wave mechanics. Examples of the kinds of trap separation behavior are shown in figure 3. The creation of multiple traps from a smaller number of beams is not even an effect of interference; the calculations for figure 3 were done by superimposing single beam optical force fields, assuming the beams are incoherent. The conclusion of this particular investigation was that for particles smaller than the beam waist in radius, two traps would form at a separation about the beam waist. For particles with radii close to the beam waist, critical phenomena, such as the formation of large numbers of traps, can occur subject to beam shape. For particles with radii larger than the beam waist, separation into multiple traps occurs at separations of roughly the beam waist plus the radius of the particle. Typically large particles will form a single extra trap between each beam.

To explore the effect of beam coherence on trapping dynamics using the old methodology, a large $N_{\max}$ was chosen such that the region of convergence contained both beams, the particle and the translation distance. Calculation times increases substantially and accuracy begins to decrease due to numerical instabilities for rotations at $N_{\max} > 90$. This method has the singular advantage that there is effectively only one beam in the calculation. Using the new method, a substantially lower $N_{\max}$ is used, but the calculation requires that the beams be translated separately and repeatedly added together just before the scattering calculation is performed.

Downloaded From: http://proceedings.spiedigitallibrary.org/ on 12/09/2015 Terms of Use: http://spiedigitallibrary.org/ss/TermsOfUse.aspx

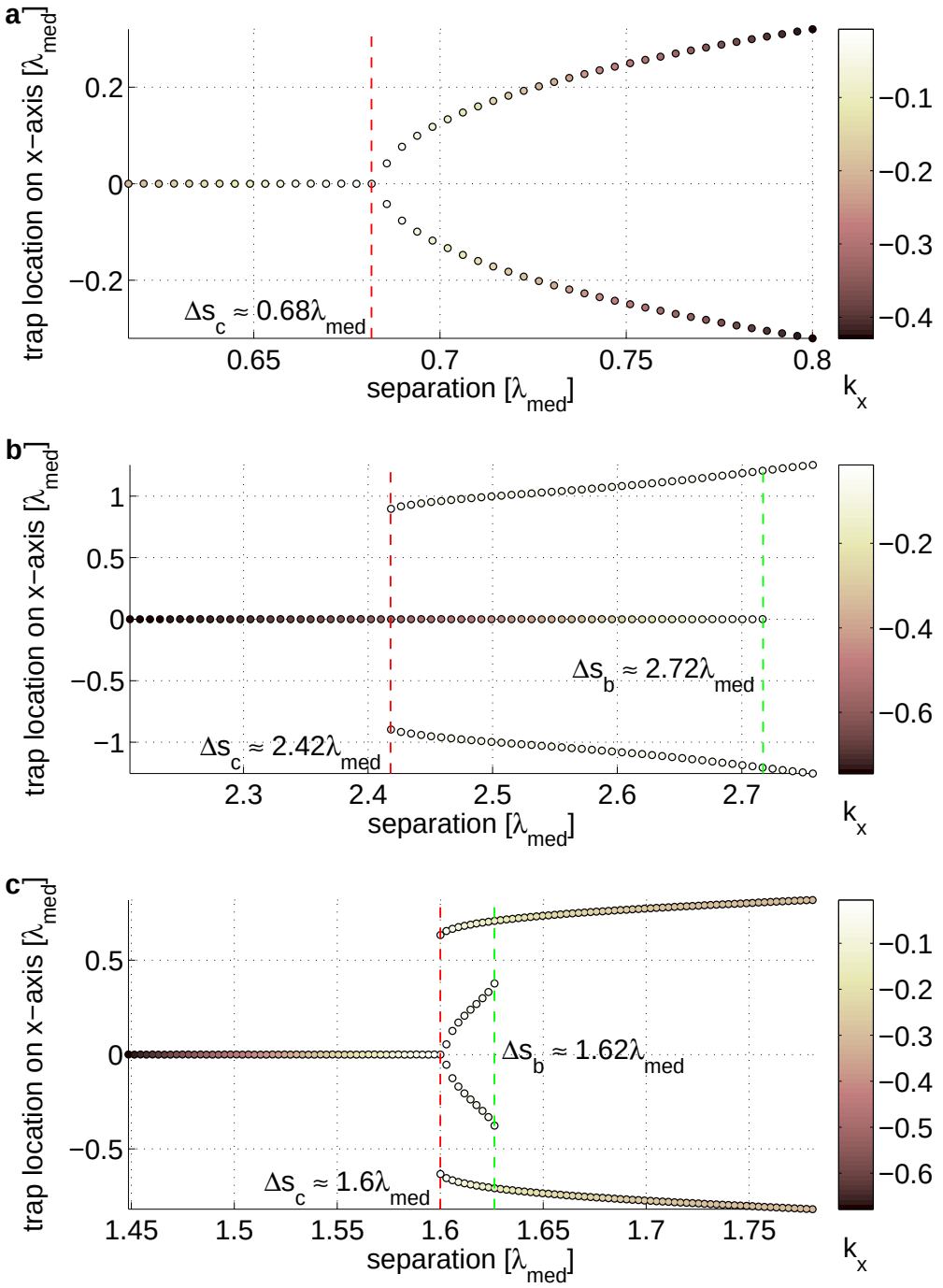

Figure 3. Representative trap locations along the z-equilibrium force contour at beam separations and particles producing: (a) two, (b) three, and (c) four traps. The color scale of the points (gray scale in printed copies) gives the local trap stiffness in the beam separation direction. (a) A $0.4\lambda_{\mathrm{med}}$ radius polystyrene particle forms two traps originating from the central trap when the critical separation, Δs_c, is reached in N.A. = 1.25 optical tweezers. (b) A silica particle of radius $1.33\lambda_{\mathrm{med}}$ in N.A. = 1.25 tweezers. The combination of force fields with a weak region of stiffness near the center followed by a larger one towards the extent of the trap generates three traps for 2.4–$2.7\lambda_{\mathrm{med}}$ separation. The separation where the original trap disappears is denoted as Δs_b. (c) Trap separations for a polystyrene particle of radius $0.88\lambda_{\mathrm{med}}$ in an N.A. = 1.3 optical tweezers calculation lead to the formation of four traps over a very small range of separations.

Downloaded From: http://proceedings.spiedigitallibrary.org/ on 12/09/2015 Terms of Use: http://spiedigitallibrary.org/ss/TermsOfUse.aspx

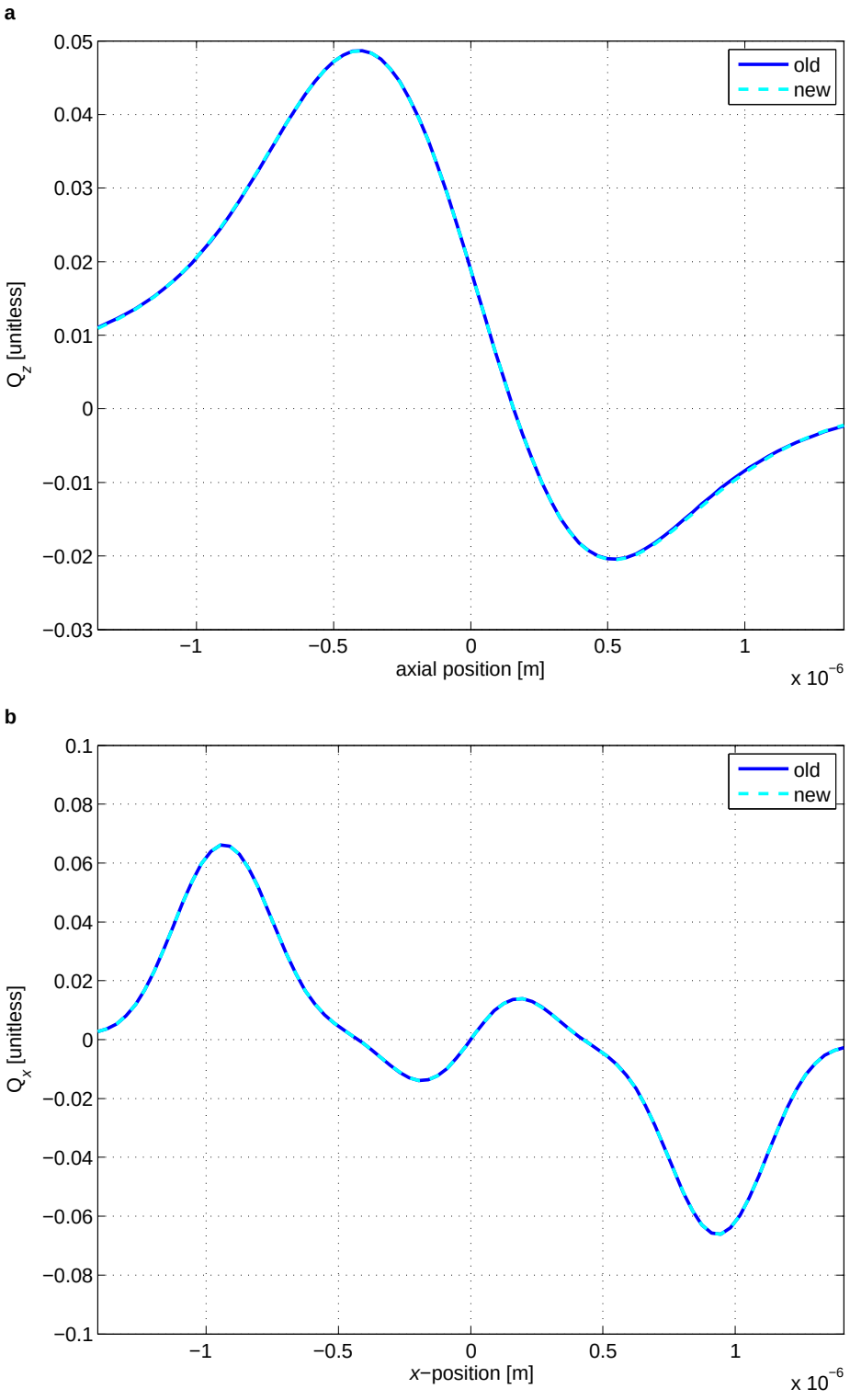

Figure 4. Overlaid force profiles for a coherent linearly polarized dual beam optical trap for the old and new methodologies in the optical tweezers toolbox. a) The axial force profile shows excellent agreement near the origin, but seems to vary slightly towards the edges of the trap. b) The profile along the x-direction (separation direction) shows excellent agreement everywhere.

Downloaded From: http://proceedings.spiedigitallibrary.org/ on 12/09/2015 Terms of Use: http://spiedigitallibrary.org/ss/TermsOfUse.aspx

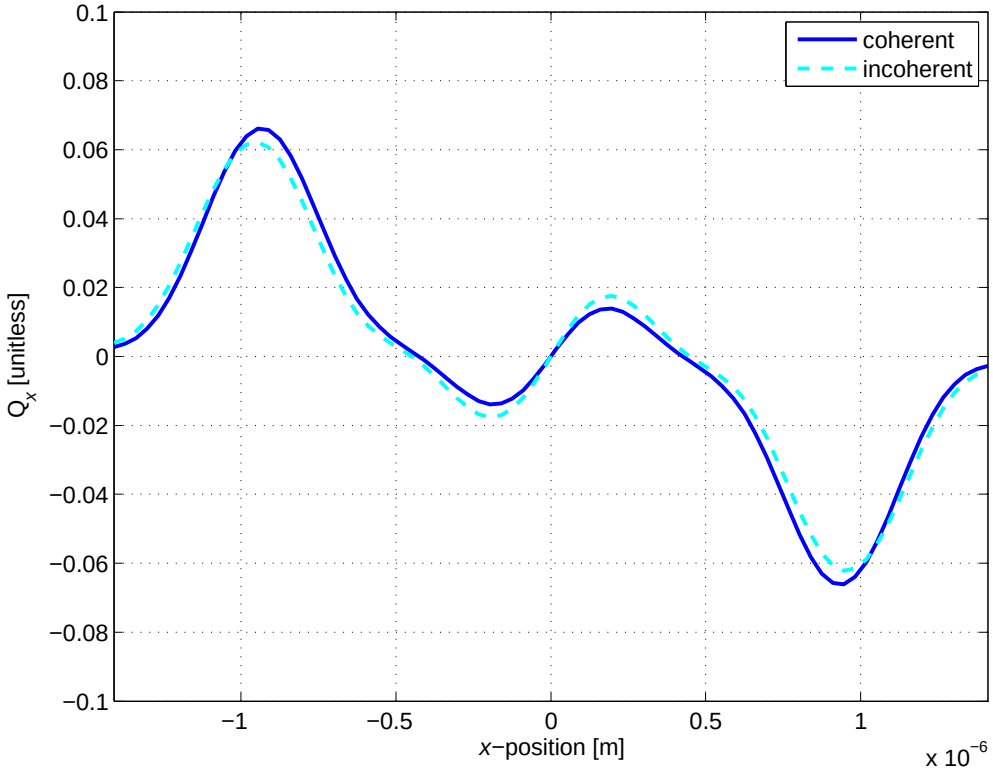

Figure 5. Overlaid force profiles for a coherent linearly polarized dual beam optical trap for coherent, in phase beams (solid line), and incoherent beams (dashed line).

Here we chose a separation of 1μm between two beams produced by a high power focusing element and a particle of $r = 0.5\mu$m. Figure 4(a) and (b) shows the outcome of the calculation for the two methods overlaid on each other along the z- and x-directions, respectively. Figure 4(a) shows the biggest difference out of the two plots in the figure. The angular momentum modes in the beam must add up to the correctly due to the conditioning of the problem so the deviation must be due to the radial functions. The radial functions are not constrained as much as the angular momentum modes because it cannot be correct everywhere except with an infinite number of basis functions. Whilst the deviation comes from the choice of truncation the difference noted here is small compared to the total force being on the order of 0.1%. Based on this data caution is advised when choosing a truncation as systematic errors can appear if the beam cannot be adequately described everywhere in space. However, it is generally sufficient for the first few radial modes to be calculated in highly focused beams.[21]

The force profiles shown in figure 4 are for coherent beams. The separation of the beams does not completely eliminate the effect of interference as it is the particle which determines how light is transformed. If there is some kind of set phase relationship between the two beams, as is the case of beams generated by an SLM, then there will be some interference effect through interaction with the particle. For multi-particle systems this can be a measurable effect, but will be greatly weakened as multiple particles tend to be held at much greater distances than the particles shown here. This can also be a problem for SLM control along the beam axis as the beam which focuses first in the path will affect the second based on their phase relationship. Interference due to this changing phase relationship will create shifts in the stable trapping positions. On the other hand, the phase relationship between the two incoherent beams is irrelevant. This indicates that changes to the stable trapping positions may appear when two coherent beams near each other.

Counter propagating beam calculations for particles in both the coherent and incoherent beams have been performed using the toolbox.[22]

A detailed mathematical model of the electromagnetic properties of materials is a boon for understanding

Downloaded From: http://proceedings.spiedigitallibrary.org/ on 12/09/2015 Terms of Use: http://spiedigitallibrary.org/ss/TermsOfUse.aspx

and characterizing optical tweezers. Calculations using a good computational model of light scattering is crucial in certain situations, such as the observation of interference effects in counter propagating and other multiple beam systems. Further, important and unexpected details, such as the formation of a number of traps greater than the number of beams can be found more easily with the computational model of the problem than the experiment.

5. DYNAMIC SIMULATION AND BROWNIAN MOTIONS IN OPTICAL TWEEZERS

Dynamic modeling of optical tweezers is the final piece of the theoretical problem of optical tweezers. The calculation of force maps for single spherical particles is an invaluable tool for characterization of simple measurement apparatus. However, as soon as other particles are added, or the geometry of the particles deviates from the spherical, the simple force field picture in the three spatial dimensions is broken. Non-spherical particles, such as ellipsoids and cylinders have optical force fields and optical torque fields—a five (six for a non-rotationally symmetric object) dimensional problem. To brute force six dimensions with current technology is not feasible. There is a solution to this problem—dynamic simulation. By moving and rotating a particle and observing the results one not only reproduces what happens in experiments, one can reproduce the low energy behavior of the system. In general, particles move along the path of least action and so calculation in this manner is not only quick, but a reasonable way to attack the problem of trap characterization.[10]

Brownian motion at low frequencies may also be of interest when looking at objects of non-spherical geometries. The equations of motion for a non-spherical particle in water at low frequencies is straight forward:

$$\mathbf{r}_{i+1} = \Gamma_{\mathrm{t}}^{-1}\mathbf{F}_i^o\Delta t + \mathbf{r}_b, \tag{10}$$

$$\boldsymbol{\omega} = \Gamma_{\mathrm{r}}^{-1}\mathbf{T}_i^o + \boldsymbol{\omega}_b, \tag{11}$$

$$\mathbf{R}_{i+1} = \Delta\mathbf{R}\mathbf{R}_i \tag{12}$$

where $\mathbf{r}$ is the position coordinate, $\boldsymbol{\omega}$ is the angular velocity, Γ_{t} the translational drag tensor and Γ_{r} the rotational drag tensor. The angular velocity becomes an incremental rotation matrix, $\mathbf{R}$, through the use of the Euler-Rodriguez formula. The optical forces, $\mathbf{F}^o$, and torques, $\mathbf{T}^o$, are calculated each time step. The normally distributed positions and angular velocities derived from the translational and rotational drag tensors are denoted $\mathbf{r}_b$ and $\boldsymbol{\omega}_b$, respectively.

It is even beneficial to calculate the dynamic action of a microsphere under Brownian motion,especially when more than one beam is present. Figure 6 shows a visualization of trapping behavior for a single approximately wavelength diameter microsphere trapped in a triangle (or ring of sorts) consisting of three incoherent beams. This kind of calculation is simple to achieve using the toolbox and the equations provided in this section. As this particle is on the order of a wavelength in diameter it displays multiple traps beyond the number of beams. Further, the "phantom" traps can easily be deeper than the native traps near the center of each beam, this is despite the fact that the force field doesn't strongly feature on the arrow plot overlaid over the Brownian motion data. As the simulation keeps all the parameters the depth, trapping volumes and other relevant features can be found. Brownian motion adds new behavior not present in the calculation of the optical force field and so one gains further insight to the optical trapping problem.[23] Understanding the behavior of such complicated systems cannot be achieved in the simple force field picture, the complexity of the data prevents an intuition by observation. As a result, looking at the scalar data of occupation through Brownian motion offers a simple way of understanding the general shape of the optical traps and transition rates between the traps. Indeed, the measurement of surface forces experienced by nanotools is vitally linked to thermal behaviors.[24]

6. MULTIPLE PLATFORM OPTICAL TWEEZERS CODE

One of our recent goals has been to produce a library of functions capable of reproducing some of the optical tweezers toolbox functionality. There are a few advantages and disadvantages to this. A big advantage is that by making a library in a generic programming language such as C++ it is possible to move the code to a wide variety of operating platforms independent of MATLAB. By putting it in library form we can make the usage

Downloaded From: http://proceedings.spiedigitallibrary.org/ on 12/09/2015 Terms of Use: http://spiedigitallibrary.org/ss/TermsOfUse.aspx

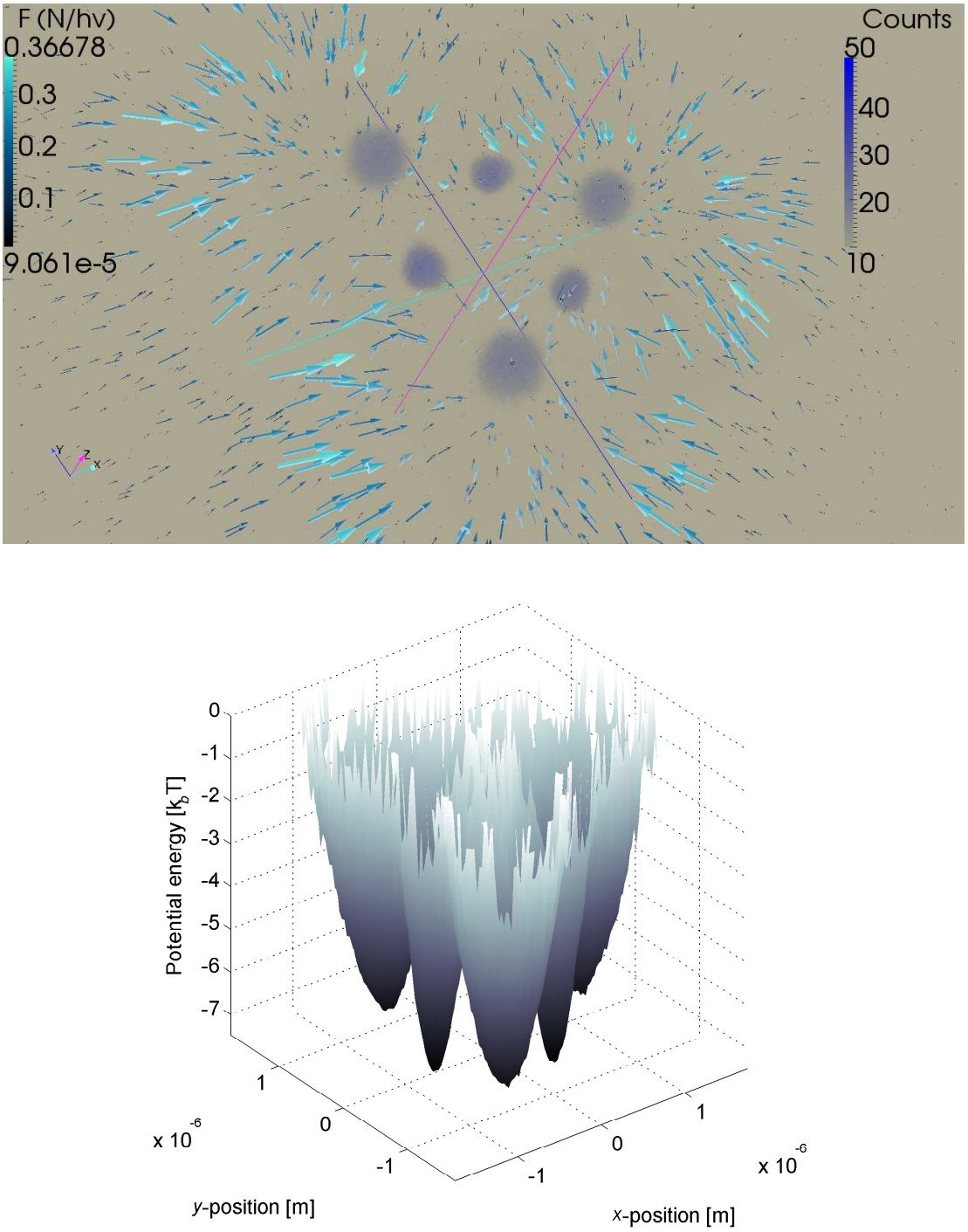

Figure 6. A representation of the trapping details of a triple beam optical trap confining a single micron sized microsphere. The top plot shows a representation of the optical force field and position density for a trapped microsphere in water. The particle stays far away from the transverse extremes, which on the plot are seen as large arrows. The particle spends significant amounts of time away from the centers of the three beam optical trap. The bottom plot shows the pseudo-potential of a slice of the occupation density for the deepest potentials which for this particle and beam separation is in the region of "phantom" optical traps between the beams.

Downloaded From: http://proceedings.spiedigitallibrary.org/ on 12/09/2015 Terms of Use: http://spiedigitallibrary.org/ss/TermsOfUse.aspx

of it as simple as possible that researchers can easily obtain useful results. As MATLAB is essentially matrix manipulation software it contains several idiosyncrasies not present in a pure programming language. MATLAB for example is at its most efficient when a store is a tensor of rank 0–2. Therefore, multidimensional problems, such as the calculation of translation coefficients is slow. Indeed, the calculation of these coefficients is one of the biggest time inefficiencies of the optical tweezers toolbox for MATLAB. However, MATLAB contains a fairly comprehensive and easy to use scripting language. It therefore is easy to both exploit plotting and special functions not present in languages such as C++. The library that has been produced for C++ contains a C wrapper for MATLAB shared-library integration plus bindings for the Python programming language*. The multiple platform tweezers library models optical tweezers for spherical scatters in arbitrary Laguerre-Gaussian beams. The library abstracts out the calculation of special functions, the basis function truncation, and the detail of how the scattering calculation is performed with beams. To use the library in its native C++ environment no detailed understanding of the mathematics is required, just some knowledge of programming to make what is effectively a script for the hard coded mathematics. Install scripts are provided for MATLAB so that the special functions can be calculated with the faster methods provided by the library and integrated in the optical tweezers toolbox.

A comparison of trapping results from both the Optical Tweezers Toolbox 1.2 and OTTCPP are displayed in figure 7. In this case a TEM_{00} beam with a truncation angle of 70° was chosen to trap the particle. The results for a 1λ radius particle of refractive index 1.5 in a medium of refractive index 1.3 between the toolbox and library compare favorably. Both match each other to a high degree over most of the range.

It should be also noted that as OTTCPP is written in C++ all the physical objects such as beams, T-matrices, rotations and translations are actual computational objects and therefore can be treated in code uniquely. Further, the modular pieces can be organized in a nearly seamless way, greatly simplifying usage. Indeed, the code used to invoke OTTCPP is in some way more user friendly than in the MATLAB implementation. The exception of course is that in general the OTTCPP needs to be compiled unless it has already been done so as an add in for MATLAB.

7. DISCUSSION AND CONCLUSION

Comparison of the old and new optical tweezers toolbox has been presented. The new methodology is more suited towards dynamic calculations and large beam separations. The new method takes advantage of the observation that beams which can be described by a small number of multipole terms (as is the case in highly focused Gaussian beams). Translation of these modes from the origin of calculation to any other point leaves the field locally correct at the new translated location. As a result, this local expansion can be acted upon by a T-matrix and yield the correct forces and torques. Emergent effects such as the creation of optical traps of number in excess of multiple beams has also been discussed as a discovery from analysis of data from the optical tweezers toolbox. Interference effects acting on trap geometry has been demonstrated and compared to optical forces arising from incoherent beams. The power of faster-than-experimental simulation of optical tweezers has also been demonstrated using Brownian motion data in three dimensions to characterize a complicated energy landscape of multiple beams. Lastly, an alternative to MATLAB and the optical tweezers toolbox has been presented in the form of a library for C++ which gives it cross platform portability. The new library has functions that allow interoperability with C and MATLAB and allows for Python integration. The biggest contrast between the Optical tweezers toolbox and the library (OTTCPP) is in how beam coefficients are determined. Beams are calculated using a point matching method in the optical tweezers toolbox and a surface integral method in OTTCPP. This is done to avoid using a linear system solver. Indeed the hybrid T-matrix method itself could be calculated using surface integrals[25] (though requiring a matrix inversion to find the coefficients) and so extend OTTCPP to objects of arbitrary shape.

*All available at http://www.physics.uq.edu.au/omg/Links.html

Downloaded From: http://proceedings.spiedigitallibrary.org/ on 12/09/2015 Terms of Use: http://spiedigitallibrary.org/ss/TermsOfUse.aspx

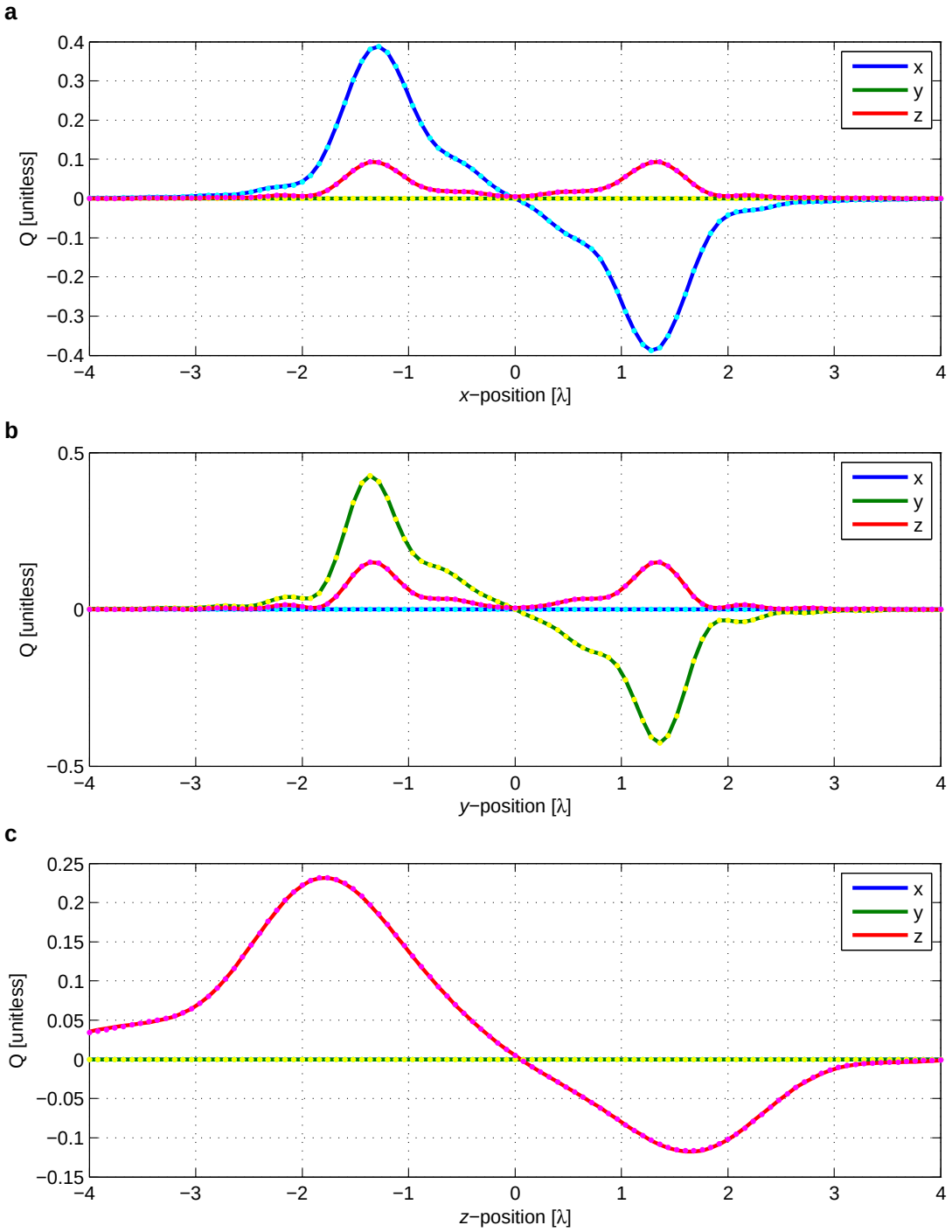

Figure 7. Normalized force efficiency (Q) as a function of position in Cartesian coordinates. Calculation from the optical tweezers toolbox appear as solid lines and calculation from OTTCPP appear as dots overlaid on the lines. Excellent correspondence between the two occur for translations in both the a) x-, b) y- and c) z-directions.

Downloaded From: http://proceedings.spiedigitallibrary.org/ on 12/09/2015 Terms of Use: http://spiedigitallibrary.org/ss/TermsOfUse.aspx

REFERENCES

[1] Ashkin, A., Dziedzic, J. M., Bjorkholm, J. E., and Chu, S., "Observation of a single-beam gradient force optical trap for dielectric particles," *Optics Letters* **11 (5)**, 288–290 (1986).

[2] Ashkin, A., "Acceleration and trapping of particles by radiation pressure," *Phys. Rev. Lett.* **24**, 156–159 (Jan 1970).

[3] Taylor, M. A., Knittel, J., Hsu, M. T. L., Bachor, H.-A., and Bowen, W. P., "Sagnac interferometer-enhanced particle tracking in optical tweezers," *Journal of Optics* **13**(4), 044014 (2011).

[4] Fällman, E. and Axner, O., "Design for fully steerable dual-trap optical tweezers," *Applied Optics* **36 (10)**, 2107–2113 (1997).

[5] Di Leonardo, R., Ianni, F., and Ruocco, G., "Computer generation of optimal holograms for optical trap arrays," *Optics Express* **15**(4), 1913–1922 (2007).

[6] Moffitt, J. R., Chemla, Y. R., Izhaky, D., and Bustamante, C., "Differential detection of dual traps improves the spatial resolution of optical tweezers," *Proceedings of the National Academy of Sciences* **77**, 9006–9011 (2006).

[7] Preece, D., Keen, S., Botvinick, E., Bowman, R., Padgett, M., and Leach, J., "Independent polarisation control of multiple optical traps," *Opt. Express* **16**, 15897–15902 (Sep 2008).

[8] Stilgoe, A. B., Heckenberg, N. R., Nieminen, T. A., and Rubinsztein-Dunlop, H., "Phase-Transition-like Properties of Double-Beam Optical Tweezers," *Physical Review Letters* **107**(24), 248101 (2011).

[9] Mazolli, A., Maia Neto, P. A., and Nussenzveig, H. M., "Theory of trapping forces in optical tweezers," *Proceedings of the Royal Society of London A* **459**, 3021–3041 (2003).

[10] Cao, Y., Stilgoe, A. B., Chen, L., Nieminen, T. A., and Rubinsztein-Dunlop, H., "Equilibrium orientations and positions of non-spherical particles in optical traps," *Opt. Express* **20**, 12987–12996 (Jun 2012).

[11] Nieminen, T. A., Loke, V. L. Y., Stilgoe, A. B., Knöner, G., Brańczyk, A. M., Heckenberg, N. R., and Rubinsztein-Dunlop, H., "Optical tweezers computational toolbox," *Journal of Optics A: Pure Applied Optics* **9**, S196–S203 (2007).

[12] Jahnel, M., Behrndt, M., Jannasch, A., Schäffer, E., and Grill, S., "Measuring the complete force field of an optical trap," *Optics Letters* **36 (7)**, 1260–1262 (2011).

[13] Lorenz, L., "Lysbevægelsen i og uden for en af plane lysbølger belyst kugle," *Videnskabernes Selskabs Skrifter* **6**, 2–62 (1890).

[14] Mie, G., "Beiträge zur Optik trüber Medien, speziell kolloidaler Metallösungen," *Annalen der Physik* **25**, 377–445 (1908).

[15] Gouesbet, G., "Generalized Lorenz-Mie theories, the third decade: A perspective," *Journal of Quantitative Spectroscopy and Radiative Transfer* **110**(14-16), 1223–1238 (2009).

[16] Mishchenko, M. I., "Light scattering by randomly oriented axially symmetric particles," *Journal of the Optical Society of America A* **8**(6), 871–882 (1991).

[17] Crichton, J. H. and Marston, P. L., "The measurable distinction between the spin and orbital angular momenta of electromagnetic radiation," *Electronic Journal of Differential Equations 4* , 37–50 (2000).

[18] Farsund, Ø. and Felderhof, B. U., "Force, torque, and absorbed energy for a body of arbitrary shape and constitution in an electromagnetic radiation field," *Physica A* **227**(1-2), 108–130 (1996).

[19] Choi, C. H., Ivanic, J., Gordon, M. S., and Ruedenberg, K., "Rapid and stable determination of rotation matrices between spherical harmonics by direct recursion," *Journal of Chemical Phyics* **111**, 8825–8831 (1999).

[20] Videen, G., [*Light Scattering from Microstructures*], no. 534 in Lecture Notes in Physics, Springer Berlin / Heidelberg (2000).

[21] Nieminen, T. A., Rubinsztein-Dunlop, H., and Heckenberg, N. R., "Multipole expansion of strongly focussed laser beams," *Journal of Quantitative Spectroscopy and Radiative Transfer* **79-80**, 1005–1017 (2003).

[22] Loke, V. L. Y., Nieminen, T. A., Heckenberg, N. R., and Rubinsztein-Dunlop, R., "Dual-beam interferometric laser trapping of rayleigh and mesoscopic particles," *Piers 2008 Hangzhou: Progress In Electromagnetics Research Symposium, Vols I and Ii, Proceedings* (2008).

[23] Sun, B., Lin, J., Darby, E., Grosberg, A. Y., and Grier, D. G., "Brownian vortexes," *Phys. Rev. E* **80**, 010401 (Jul 2009).

[24] Phillips, D. B., Grieve, J. A., Olof, S. N., Kocher, S. J., Bowman, R., Padgett, M. J., Miles, M. J., and Carberry, D. M., "Surface imaging using holographic optical tweezers," *Nanotechnology* **22**(28), 285503 (2011).

[25] Waterman, P. C., "Symmetry, unitarity, and geometry in electromagnetic scattering," *Phys. Rev. D* **3**, 825–839 (Feb 1971).

Downloaded From: http://proceedings.spiedigitallibrary.org/ on 12/09/2015 Terms of Use: http://spiedigitallibrary.org/ss/TermsOfUse.aspx